Soft Matter

Dynamic Article Links

Cite this: *Soft Matter*, 2012, **8**, 8582

www.rsc.org/softmatter

PAPER

Capillary interactions among spherical particles at curved liquid interfaces

Chuan Zeng,[a] Fabian Brau,[b] Benny Davidovitch[a] and Anthony D. Dinsmore[a]

Received 13th April 2012, Accepted 29th May 2012
DOI: 10.1039/c2sm25871d

We study the effect of interfacial curvature on the binding energy and forces exerted on small spherical particles that adsorb on an interface between two immiscible liquids. When the interface has anisotropic curvature, the constant-contact-angle condition at the particle-fluid boundary requires a deformation of the interface. Focusing on the case of an initially cylindrical interface, we predict the shape after a spherical particle binds. We then calculate the energy of adsorption and find that it depends on the shape of the interface very far from the binding site. Turning to the problem of two adsorbed spherical particles, we predict a capillary interaction that arises purely from the deformations caused by the contact-angle condition. An analogy is made between these curvature-induced capillary forces and electrostatic forces between quadrupoles in two dimensions. We conclude with a conjectured general form for the interaction of a single spherical particle with the Gaussian curvature of the underlying fluid interface, which we compare to previous work.

I. Introduction

Particles adsorbed on interfaces between immiscible fluids play an important role in a variety of technological applications and raise a number of fundamentally interesting questions. Solid, microscopic particles are used to stabilize droplets in Pickering emulsions in foods, cosmetics, and oil recovery.[1–7] In materials science, monolayers of nanoparticles or micron-sized particles are studied as a means to form functional membranes or capsules.[8–17] In these cases, the adsorption of particles on the liquid interface is driven by a reduction of the total interfacial energy, provided that the particle does not strongly favor one liquid over the other.

In the continuum approximation where the particle is much larger than the molecular scale, the molecular interactions among the particles and the two liquids are described in terms of three interfacial tensions: γ (liquid–liquid), γ_1 (particle and liquid I), and γ_2 (particle and liquid II). Assuming that the particle is spherical and uniform (*i.e.*, does not pin the contact line), its binding energy to a planar interface can be written as a simple function of the particle radius a and γ, γ_1, and γ_2.[18,19] This model also predicts that the angle of contact (θ_c) between the sphere and the interface remains constant and its value is given by the Young–Dupré equation, $\cos\theta_c = (\gamma_1 - \gamma_2)/\gamma$. Thus, in the absence of gravity the interface remains planar and the particle simply inserts itself partially into the interface. Such spheres would not be subject to forces in the direction tangential to the interface. On the other hand, when the spheres are electrostatically charged or subject to gravity, the interface is deformed near the particle and tangential forces arise.[20–32] In many relevant cases, these forces act over distances much larger than the particle size because constraints on the interfacial shape often imply that deformations extend over long range. Hence, geometric constraints and interfacial deformations play an important role in the mechanics of adsorbed particles. As an example of the importance of geometry, when *non*-spherical particles adsorb at a planar interface, the constant-θ_c condition requires that the interface be deformed.[33–36] This deformation gives rise to tangential torques and forces on the particles even when gravity is irrelevant (*e.g.*, when the particles and fluids are density-matched). In a similar fashion, spherical particles in which the contact line is pinned (so that θ_c is not uniform) are also subject to tangential capillary forces.[34,37,38]

In many relevant cases, however, fluid interfaces are not planar and the geometry of the interface must be considered more carefully. Anisotropy of the interfacial shape can be induced by gravity, applied electric fields, or by contact forces among droplets in an emulsion. Even in the absence of external forces, anisotropy of the interface shape can arise from contact with a solid surface. Examples include droplets adhered to fibers or stretched between two interfaces. These cases are relevant in printing or deposition on surfaces, nucleation of liquids on MEMS devices, or manipulation of fabricated micro- or nano-devices on liquid interfaces.[39,40] In any of these cases, the constant-θ_c condition can deform the interface and the binding energy of a spherical particle may be substantially different from the planar-interface case. Moreover, non-uniformity in the interface shape may lead to strong capillary forces in the tangential direction.

[a]*Physics Department, University of Massachusetts, Amherst, MA 01003, USA*
[b]*Laboratoire Interfaces et Fluides Complexes, Université de Mons, Place du Parc 20, BE-7000 Mons, Belgium*

In this article, we address the problem of adsorption of one or more spherical particles on a fluid interface that is initially curved in an anisotropic shape. Specifically, we study the effect of the interfacial curvature on the binding energy and on the associated capillary force exerted on the particles.

The focus of our study, which allows the derivation of analytic expressions for the energy and the force, is the simplest case of an anisotropic uniform interface: an infinitely long cylinder that is deformed due to the adsorption of one or two small spherical particles. We find that the energy of adsorption is finite but depends on the induced long-range deformation of the interface far away from the adsorbed particle. This implies that although the assumption of a nearly flat interface gives a reasonable approximation of the interface deformation near the particle, it is not sufficient to compute the binding energy. In contrast, we find that the interaction between two adsorbed particles does not necessarily depend on the long-range interfacial deformation. Our calculation suggest that the capillary force exerted on a small spherical particle is given by a formula that depends only on the local interfacial geometry:

$$\boldsymbol{F}(\boldsymbol{r}) = -(\pi/6)\gamma a^4 \sin^4 \theta_c \nabla G_0(\boldsymbol{r}), \tag{1}$$

where $\boldsymbol{r}$ is the particle position, a is the particle radius and $G_0(\boldsymbol{r})$ is the Gaussian curvature of the unperturbed interface. The interaction between the two adsorbed particles is described by eqn (1) as long as they are separated by a distance that is much larger than a but much smaller than the radius of curvature of the interface.

Our paper adds new elements to a previous calculation by Würger, who studied a spherical particle on a catenoid: an interface that has zero mean curvature H and negative Gaussian curvature (*i.e.*, a saddle-like shape).[41] Comparison of our results with Würger's study enables us to conclude with a general discussion of the roles of G and H on the interactions between adsorbed particles, and to conjecture that the force equation (eqn (1)) should apply generally for a spherical particle on any fluid interface of constant mean curvature H.

This article is organized as follows: In Section II we review the basic theory of particle adsorption at a liquid interface and introduce a general formalism that allows us to calculate interface-mediated binding energies and forces on small adsorbed spherical particles through an appropriate linear differential (local) operator. The coefficients of this operator depend on the Gaussian curvature and mean curvature of the undisturbed interface. In Section III we specialize to the deformation of a fluid cylinder due to an adsorbed spherical particle and discuss a useful analogy to quadrupolar electrostatic fields. We then use the deformation to find the curvature correction to the *binding energy*, showing its nonlocal nature. In Section IV, we employ the deformation of the cylindrical interface to derive a general formula for the *tangential force* exerted on a particle adsorbed on a curved interface. Since the azimuthal and translational invariance of the cylinder exclude any net force on one adsorbed spherical particle, we first break this undesirable symmetry by placing another small particle on the cylinder, and then compute the forces between the two particles. In Section V we compare our results to previous studies, comment on the relevance of this theoretical study for specific physical systems, and draw some general conclusions.

II. General formalism: small particle adsorbed onto on a curved interface

In this section, we review the classical problem of a solid spherical particle of radius a that is brought to contact with an infinite and planar interface between two immiscible liquids (Fig. 1). To set the ground for addressing interface curvature effects, we then briefly review basic concepts of differential geometry of surfaces and recall Laplace's law that connects the pressure and mean curvature of an interface. Following this short exposition, we introduce a linear operator whose coefficients depend on the Gaussian and mean curvature of the undisturbed interface. This operator allows us to describe interfacial deformations that preserve a uniform (constant) pressure at the interface. We then discuss the deformation of a generic fluid interface by an adsorbed particle.

A. Adsorption on a planar interface

To address the problem of a spherical particle at a planar liquid interface, we follow the arguments of Koretsky and Kruglyakov[19] and Pieranski.[18] The particle will adsorb onto the fluid interface if the total interfacial energy (associated with I–II, particle-I, particle-II contacts) is lowered by forming a finite contact area between the fluid phases. We assume that the particle is initially in phase I and becomes partially immersed in II. The change in total interfacial energy is composed of three terms, which describe the reduction of I–II and particle-I contact areas and the energy of forming a particle-II contact. Minimizing with respect to the distance between the sphere and the interface, one finds that the "binding energy" ΔE is negative (favorable for binding) if $|\cos \theta_c| < 1$ where θ_c is the Young–Dupré contact angle:

$$\cos \theta_c = (\gamma_1 - \gamma_2)/\gamma. \tag{2}$$

In this case,[18]

$$\Delta E = -\pi a^2 \gamma (1 + \cos \theta_c)^2. \tag{3}$$

In this planar-interface example, the spherical particle simply punches a hole in the interface and adjusts its height so as to satisfy the contact-angle condition; there is no deformation of the interface.

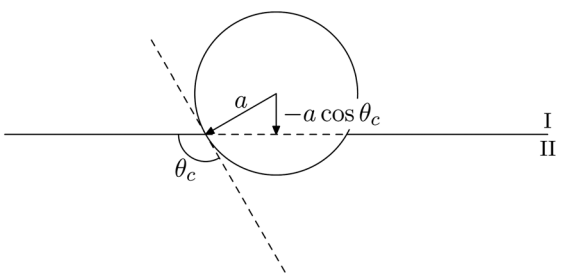

Fig. 1 Illustration of a spherical particle at a flat interface, showing the definition of the contact angle θ_c. Mechanical equilibrium requires a constant θ_c around the entire contact ring. Because of the axial symmetry, this condition is satisfied on a planar or spherical interface simply by setting the appropriate immersion depth.

The problem we tackle in this paper is this: how is the above scenario modified when the fluid interface is curved? Specifically, we ask how the binding energy and the associated tangential force are affected by the interface curvature. In order to address this question, we introduce first a few basic concepts of differential geometry that are used to describe curved surfaces.

B. Differential geometry and surface perturbations: basic concepts

The local geometry at any point $\boldsymbol{x}$ on a surface $\mathscr{S}$ is characterized by two principle curvatures $\kappa_1(\boldsymbol{x})$, $\kappa_2(\boldsymbol{x})$. The mean curvature H and Gaussian curvature G are, respectively:

$$H(x) = \frac{1}{2}[\kappa_1(x) + \kappa_2(x)] \text{ and } G(x) = \kappa_1(x)\kappa_2(x). \quad (4)$$

Laplace's law states that the pressure difference Δp at any point $\boldsymbol{x}$ of a fluid interface is $\Delta p(\boldsymbol{x}) = 2\gamma H(\boldsymbol{x})$.[42,43] In equilibrium and in the absence of gravity or other external fields, the pressure must be uniform, and therefore fluid interfaces must be surfaces of constant mean curvature (CMC).

Let us consider now the effect of a small particle that is adsorbed on a fluid interface. Prior to adsorption the interface has an "unperturbed" shape $\mathscr{S}_0$ of a CMC surface characterized by a mean curvature H_0. After adsorption and equilibration, the interface assumes a perturbed shape $\mathscr{S}_1$ which, owing to Laplace's law, must also be a CMC surface, albeit with mean curvature H_1. (Note that $H_1 = H_0$ if the pressure difference between the two fluids is held constant.) Noticing the natural dimensionless variable aH_0, we establish our analysis on perturbation theory, assuming that

$$\delta H \equiv \frac{H_1 - H_0}{H_0} \to 0 \text{ as } aH_0 \to 0. \quad (5)$$

We describe the perturbation of the interface as:

$$\boldsymbol{x} \to \boldsymbol{x} + \zeta(\boldsymbol{x})\hat{\boldsymbol{n}}(\boldsymbol{x}), \quad (6)$$

where $\hat{\boldsymbol{n}}(\boldsymbol{x})$ is the unit normal to the surface $\mathscr{S}_0$ at $\boldsymbol{x}$. For a small adsorbed particle, namely $aH_0 \ll 1$, we expect that $\zeta(\boldsymbol{x}) \sim aH_0$ since it must vanish in the absence of an adsorbed particle ($a \to 0$), and also for a planar interface ($H_0 \to 0$). The discussion in the next section will clarify the actual dependence of $\zeta(\boldsymbol{x})$ on the relevant length scales in this problem.

We seek $\zeta(\boldsymbol{x})$, from which we obtain an expression for the binding energy ΔE similar to eqn (3). This calculation is facilitated by recalling a linear differential operator that describes the perturbation (to $O(aH_0)$) of the mean curvature $\delta H(\boldsymbol{x})$ due to a normal deflection $\zeta(\boldsymbol{x})$:

$$\delta H(x) = \mathscr{L}\zeta(x),$$

$$\mathscr{L} \equiv -\left[2H_0^2 - G_0(x)\right] + \nabla_{\mathscr{S}} B(x)\cdot\nabla_{\mathscr{S}} - \frac{1}{2}\nabla_{\mathscr{S}}^2,$$

$$B(x) \equiv \frac{1}{8}\ln\left[H_0^2 - G_0(x)\right], \quad (7)$$

where $\nabla_{\mathscr{S}}$ is the gradient operator projected on the (unperturbed) surface.[44] The perturbations that we are addressing here preserve the CMC nature of the interface and hence: $\delta H(\boldsymbol{x}) = \mathscr{L}\zeta(\boldsymbol{x}) =$ const ($= 0$ if the pressure difference between the two fluids is held fixed). In Appendix A we show how $\mathscr{L}$ is derived for the special case of a cylinder.

Before proceeding, it is useful to consider two elementary examples:

(a) The first example has been addressed already in the above subsection: a particle adsorbed on an (infinite) planar surface, where both $\mathscr{S}_0$ and $\mathscr{S}_1$ are planar, hence $H_0 = \delta H = 0$ (and also $G_0 = 0$ and $\nabla_{\mathscr{S}} B = 0$ everywhere). The small parameter $aH_0 = 0$, hence the deformation vanishes ($\zeta = 0$), and the only difference between $\mathscr{S}_0$ and $\mathscr{S}_1$ is the circular hole of radius $a\sin\theta_c$ in $\mathscr{S}_1$ due to the immersed particle.

(b) Another example is a particle adsorbed on a spherical drop of radius $R \gg a$. Here, $\mathscr{S}_0$ is a sphere with $H_0 = 1/R$ and $G_0 = 1/R^2$. The perturbed surface $\mathscr{S}_1$ is a punctured sphere whose radius is computed by invoking conservation of liquid volume: $R[1 + O(a^3/R^3)]$, hence $\delta H \sim -O(a^3/R^4)$ and $\zeta(\boldsymbol{x}) \sim O(a^3/R^2)$.[45,46]

C. Deformation of a generic fluid interface by an adsorbed particle

In both examples above the deflection $\zeta(\boldsymbol{x})$ is uniform. This trivial type of deflection is enabled because the *axial symmetry* of $\mathscr{S}_0$ (around the vertical axis in Fig. 1) is preserved by the adsorbed particle. This suggests that nontrivial interfacial curvature effects may appear in interfaces that do not possess such axisymmetry. In such (generic) cases the perturbation $\zeta(\boldsymbol{x})$ is not constant, and it is useful to discuss its general nature. The following discussion suggests that the deformation of a generic CMC interface due to an adsorbed particle has the form:

$$\zeta(\boldsymbol{x}) = a^2 H_0 f(\boldsymbol{x}H_0; aH_0), \quad (8)$$

where f is a dimensionless function of the dimensionless variable $\tilde{\boldsymbol{x}} = \boldsymbol{x}H_0$, whose magnitude (*e.g.* $\max f(\boldsymbol{x})$) is expected to be $O(1)$ (in the limit $aH_0 \to 0$) for a generic CMC surface, and whose functional form exhibits a strong dependence on aH_0. Referring to the example in the previous section, we note that $f \sim aH_0$ for a spherical surface. The discussion below does not exclude the possibility of the more general form, $\zeta \sim a(aH_0)^\beta f(\boldsymbol{x}H_0; aH_0)$, where $\beta > 0$. However, the examples addressed in this article and the expectation of an analytic expansion about $aH_0 = 0$ suggest that $\beta = 1$.

Our derivation of eqn (8) begins by noticing that the system (particle + interface) consists of two distinct scales a and H_0^{-1}, with $a \ll H_0^{-1}$. Noticing the linear nature of the operator $\mathscr{L}$ and recalling the general theory of linear response to localized perturbations (Green's function), one may naively assume that the *amplitude* of $\zeta(\boldsymbol{x})$ depends only on a (the typical "scale of perturbation"), whereas the *spatial variation* of the perturbation $\zeta(\boldsymbol{x})$ is determined only by H_0^{-1} (the typical "scale of operator $\mathscr{L}$"). Nevertheless, although the perturbation induced by an adsorbed particle is localized (since $a \ll H_0^{-1}$), it is not a point impulse. This is in contrast to basic applications of Green's theory. We will argue below that this fact leads to the deformation type expressed mathematically in eqn (8): a perturbation whose amplitude $\sim a^2 H_0$, that is characterized by a variation on the "local" scale a and on the "global" scale H_0^{-1}.

In order to prove this, let us introduce first a dimensionless set of variables that reflect the existence of two separate scales in our

problem. A natural scale for the shape perturbation in the normal direction is the particle radius a, and a characteristic scale for variations in the tangential direction is H_0^{-1}. Let us consider now two distinct scale transformations:

(i) Firstly, assume a rescaling *of space* ($\boldsymbol{x} \in R^3$): $\boldsymbol{x}' = k\boldsymbol{x}$. In particular, this will transform the spherical particle of radius a to one with radius $a' = ka$. Similarly, the surface $\mathscr{S}_0$ will transform to $\mathscr{S}_0'$ such that: $H_0' = H_0/k$; $G_0'(x') = G_0(x)/k^2$. It follows that $\zeta'(\boldsymbol{x}', a') = k\zeta(\boldsymbol{x},a)$. Notice that this affine transformation satisfies: $aH_0 = a'H_0'$. This suggests that the perturbation can be written as: $\zeta(\boldsymbol{x})/a = \tilde{\zeta}(\boldsymbol{x}H_0; aH_0)$, where $\tilde{\zeta}$ is a dimensionless function that depends on the dimensionless variable $\boldsymbol{x}H_0$ and the dimensionless parameter aH_0. The nature of the function $\tilde{\zeta}$ is further elucidated by considering the following transformation.

(ii) Consider now a rescaling *of the surface* $\mathscr{S}_0$ ($\boldsymbol{x} \in \mathscr{S}_0$): $\boldsymbol{x}'(\boldsymbol{x})$, such that $H_0' = H_0/k$; $G_0'(\boldsymbol{x}') = G_0(\boldsymbol{x})/k^2$ but $a' = a$. Notice that for this non-affine transformation $a'H_0' \neq aH_0$. As $k \to \infty$ (and $aH_0 \to 0$), the surface becomes flatter and flatter, and we expect that the problem reduces to example (a) in the previous section: a (finite) particle adsorbed on a planar interface, where $\zeta/a = 0$. This suggests that $\tilde{\zeta} \sim aH_0$ and leads to eqn (8), which implies that for generic surfaces, $\zeta(\boldsymbol{x})/a$ is expected to reach a vanishing amplitude in the limit $aH_0 \to 0$.

In technical language, eqn (8) stems from the fact that, although the linear operator $\mathscr{L}$ of eqn (7) is *regular*, the small adsorbed particle implies a *singular* perturbation (hence the explicit dependence of $f(\boldsymbol{x})$ on aH_0 in this asymptotic limit). In contrast to a point force (which underlies Green's function), an adsorbed particle implies a boundary condition (BC) along a boundary whose size is finite ($\sim a$).

To summarize this section, we formulated and discussed the problem of a solid spherical particle that is adsorbed to a general curved interface and hypothesized that the deformation must scale as in eqn (8). We use this formalism in the following section to analyze the deformation of a cylindrical interface by an adsorbed particle.

III. A particle adsorbed on a cylindrical fluid interface

The simplest interface on which the adsorption of a spherical particle breaks axial symmetry, and hence causes a nonuniform perturbation, is an infinitely long cylinder (Fig. 2). This section is dedicated to adsorption of a single particle on a cylinder. We start by showing that eqn (7) for the perturbation reduces to the Helmholtz equation and derive the boundary conditions that are imposed by the adsorbed particle. Then we solve the Helmholtz equation with approaches commonly used in electrostatic problems, and use this solution to find the binding energy of a particle on a cylinder. The breaking of axisymmetry and the consequent nonuniform perturbation of the cylinder are illustrated in Fig. 4 and 6. In Section IV, we consider adsorption of two particles on a cylinder to address the curvature-induced particle–particle interactions.

A. Helmholtz equation and boundary conditions

We use a cylindrical coordinate system, in which the z-axis extends along the cylinder's length, θ is along the circumferential direction, and r is the radial distance from the z-axis to the interface (see Fig. 2). When introducing dimensionless coordinates, we choose for convenience to rescale tangential (interfacial) lengths by $R = H_0^{-1}/2$, such that:

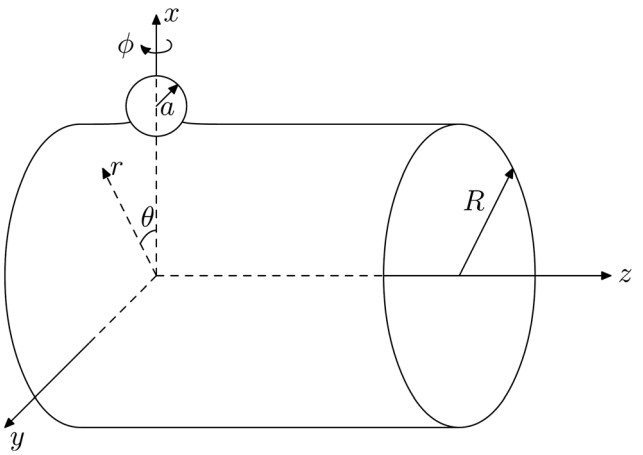

Fig. 2 A section of an infinitely long cylinder of radius R with a particle of radius a immersed on its surface. Owing to the broken symmetry around the x-axis, the interface is deformed.

$$\tilde{z} = z/R;\ \tilde{r} = r/R;\ \tilde{\zeta} = \zeta/a;\ \delta \equiv a/R. \tag{9}$$

Our rescaling of the interface deformation ζ is motivated by eqn (8). With these dimensionless variables, the unperturbed surface is $\mathscr{S}_0 := \{\tilde{\boldsymbol{x}} = (\tilde{r} = 1,\theta,\tilde{z})\}$, and the perturbed surface is $\mathscr{S}_1 := \{\tilde{\boldsymbol{x}} = (1 + \tilde{\zeta}(\theta,z),\theta,\tilde{z})\}$. Since the cylinder is of infinite volume, we expect that the mean curvature is unperturbed by the adsorption of a particle, hence $\delta H = 0$. Finally, for the (unperturbed) cylinder $G_0 = 0, \nabla_{\mathscr{S}} B = 0, H_0 = 1/(2R)$, and eqn (7) and (8) become:

$$0 = f + (\partial_{\tilde{z}}{}^2 f + \partial_{\theta}{}^2 f), \tag{10}$$

where the deformation $\tilde{\zeta}$ is:

$$\tilde{\zeta} = \zeta/a = \delta f(\theta,\tilde{z}), \tag{11}$$

according to eqn (8). This is the well-known Helmholtz equation (see Appendix A). The first term of eqn (10) corresponds to change of the mean curvature arising from a uniform expansion or dilation of the cylinder (constant f).

1. Boundary shape. Eqn (10) shows that our problem can be naturally mapped from the cylindrical surface to a flat strip, parameterized with $\theta,\tilde{z}$. The strip has infinite length ($-\infty < \tilde{z} < \infty$) and finite width ($-\pi \leq \theta \leq \pi$). This is illustrated in Fig. 3. The adsorbed particle "punctures" a region around the center of this strip ($\tilde{z} = \theta = 0$), whose form will be found here. In order to do so, it is useful to recall again the non-affine transformation (8) that allows us to consider the limit $\delta \to 0$ where the cylinder becomes asymptotically flat. The example of the flat interface (Fig. 1 and example (a) of Section II) suggests that the center of the adsorbed particle is located at:

$$r_c = R[1 - \delta\cos\theta_c + o(\delta)], \tag{12}$$

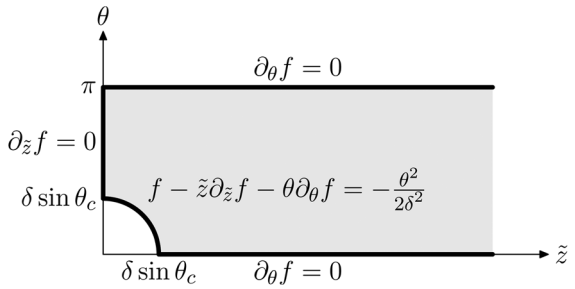

Fig. 3 Boundary conditions for the Helmholtz eqn (10). The first quadrant of the $(\tilde{z},\theta)$ coordinate system is represented as a flat plane. The center of the particle is positioned at the origin. The contact line is approximately a circle with radius $a\sin\theta_c$. As described in the text, the boundary condition at contact is obtained from the contact-angle constraint. The boundary conditions at $\tilde{z} = 0$, $\theta = 0$ and $\theta = \pi$ are determined by the mirror symmetries.

where $o(\delta)$ refers to terms that vanish faster than δ as $\delta \to 0$. The particle-interface contact line can thus be associated with the intersection of a cylinder (of radius R) with a particle of radius a whose center is at distance r_c from the cylinder axis. Moving back to our dimensionless variables, simple algebra shows that, to leading order in δ, the contact line is a circle:

$$\tilde{z}^2 + \theta^2 = \delta^2 \sin^2\theta_c + O(\delta^3). \tag{13}$$

Hence, the domain of eqn (10) is the infinite strip without a circle of radius $\delta\sin\theta_c$ around the center ($\tilde{z} = \theta = 0$).

2. Boundary conditions. The boundary conditions (BC) for our problem are shown in Fig. 3. Let us explain them, one by one:

• The crucial BC, which reflects the breaking of axisymmetry and the consequent nonuniformity of the perturbation, is along the circle of contact, eqn (13). Fixing the angle between the perturbed surface $\mathscr{S}_1$ and the particle to the contact angle θ_c, eqn (2) yields the Robin BC (Appendix B):

$$f - \tilde{z}\partial_{\tilde{z}} f - \theta\partial_\theta f = -\frac{\theta^2}{2\delta^2} \text{ on } \tilde{z}^2 + \theta^2 = \delta^2 \sin^2\theta_c. \tag{14}$$

We note that the contact angle θ_c appears implicitly in the values of $(\tilde{z},\theta)$ that define the contact ring.

• "Periodicity" in the θ-direction and mirror symmetry ($\theta \to -\theta$) imply that the problem can be restricted to one half of the strip (say, $0 \le \theta \le \pi$) with the Neumann BCs:

$$\partial_\theta f = 0 \text{ on } \theta = 0, \tag{15}$$

$$\partial_\theta f = 0 \text{ on } \theta = \pi. \tag{16}$$

Furthermore, our system is also invariant to reflections about the θ-axis ($\tilde{z} \to -\tilde{z}$). Therefore, the problem can be restricted to one quadrant (say, upper right) with the additional Neumann BC:

$$\partial_{\tilde{z}} f = 0 \text{ on } \tilde{z} = 0. \tag{17}$$

• The BCs at $\tilde{z} \to \pm\infty$ are associated with a small ($o(\delta)$) shift of the elevation of the center of the particle from the asymptotic level of the cylinder. This shift is undetermined at this stage; later in this section we will see that it is determined from energy minimization.

B. The electrostatic analogy

The similarity of eqn (10) to the Laplace equation and the BCs ((15) and (17)) suggest an analogy between the electrostatic potential in two dimensions from a quadrupolar charge distribution and the deformation of a cylindrical interface by a spherical adsorbed particle. Würger has pointed out this analogy in the problem of a spherical particle on a catenoid-shaped interface.[40] In order to see this analogy, let us consider eqn (10), ignore the term f, assume that both coordinates $-\infty < \theta,\tilde{z} < \infty$ (*i.e.* ignoring the BC (16)), and notice that the BCs ((15) and (17)) describe the electrostatic potential of a quadrupole. The similarity between the equation underlying deformation of CMC surfaces and electrostatic potential has already been noted in the literature.[30,35,38,47–50] Therefore, it may not be surprising that the interface deformation induced by a small adsorbed particle is similar to the electrostatic potential induced by a localized charge distribution. Furthermore, symmetry arguments motivate the relevance of the electrostatic quadrupole to our problem. Similar to quadrupolar charge distribution that breaks radial (axial) symmetry but retains reflection symmetry with respect to two orthogonal axes, the deformation of a cylindrical interface due to an adsorbed spherical particle is invariant under $\theta \to -\theta$, and $\tilde{z} \to -\tilde{z}$ (see Section III A 2).

This analogy allows us to derive an asymptotically exact solution to the interface deformation (in the limit $\delta \to 0$). The effect of the BCs ((15)–(17)) is accounted for by the images technique: placing a series of quadrupoles along the θ axis to satisfy all BCs simultaneously. Notably, while the images method is frequently used in electrostatics, it is not limited to solving Laplace's equation, but rather any linear homogenous partial differential equation, in particular our Helmholtz equation. Ignoring first BCs (16), the solution to the Helmholtz equation is:

$$f_0 = -\frac{\pi}{48}\delta^2 \sin^4\theta_c \left[J_2(\tilde{\rho}) + Y_2(\tilde{\rho})\right]\cos 2\phi, \tag{18}$$

where $\tilde{\rho} = \sqrt{\tilde{z}^2 + \theta^2}$, $\phi = \arctan(\theta/\tilde{z})$, and J_2, Y_2 are the Bessel functions (of order 2) of the first and second kind, respectively. The function $Y_2(\tilde{\rho})$ is dominant in the vicinity of the adsorbed particle (*i.e.* $\tilde{\rho} \to \delta$), but $J_2(\tilde{\rho})$ is necessary to assure decay of the deformation as $\tilde{\rho} \to \infty$. Adding the series of images we obtain the deformation that also satisfies BC (16):

$$f = -\frac{\pi}{48}\delta^2 \sin^4\theta_c \sum_{n=-\infty}^{\infty} \left[J_2(\tilde{\rho}_n) + Y_2(\tilde{\rho}_n)\right]\cos 2\phi_n, \tag{19}$$

where $\tilde{\rho}_n = \sqrt{\tilde{z}^2 + (\theta + 2n\pi)^2}$, $\phi_n = \arctan[(\theta + 2n\pi)/\tilde{z}]$. By this procedure, we guarantee that the infinite sum in eqn (19) satisfies the following properties: (i) it converges for all $\theta,\tilde{z}$. (ii) It satisfies the BC (14) at the contact line in the asymptotic limit $\delta \to 0$. These properties were verified numerically by comparing eqn (19) to direct numerical solution of eqn (10) with BCs (14)–(17), obtained by the MATLAB Partial Differential Equation (PDE) Toolbox (MathWorks Inc.). Next we discuss some key features of the deformed shape that is expressed in eqn (19).

C. The deformed cylinder

We start by discussing the local deformation, near the contact line, and then proceed to the impact of the adsorbed particle on the global shape, away from the contact line.

1. Local deformation. In the vicinity of the particle, $\tilde{\rho} \sim O(\delta)$. In this regime, both the "Helmholtz term" (f in eqn (10)) and BC (16) have negligible effect. Hence, the short-range deformation is essentially identical (to leading order in δ) to a quadrupolar electrostatic potential (Fig. 4), and originates from a Taylor expansion of the leading contribution to the deformation, $Y_2(\tilde{\rho})$:

$$f_{\text{near}} = \frac{\delta^2 \sin^4 \theta_c}{12} \frac{\cos 2\phi}{\tilde{\rho}^2} + O(\delta^2), \tag{20}$$

where the last term refers to corrections that nowhere exceed $O(\delta^2)$ (in contrast to the first term which becomes $O(1)$ at the contact line). One may notice that f reaches its maximum value at two points on the contact line ($\tilde{\rho} = \delta, \phi = 0, \pi$) (Fig. 4). Eqn (20) shows that this value is indeed $O(1)$, as was anticipated in the general discussion in Section II C (see eqn (8)).

To understand intuitively how the deformation of Fig. 4 arises from the θ_c condition, we illustrate the contact angles along the $\hat{z}$ and $\hat{\theta}$ directions for a neutrally wetting sphere ($\theta_c = 90°$). Fig. 5(a) shows the intersection of the sphere and the cylinder along the axial and circumferential directions if the center of the sphere were placed at the interface with no deformation. In this case, the contact angle is 90° in the side view (along $\hat{z}$) but is acute (<90°) in the end view ($\hat{\theta}$ direction). If the sphere is lifted slightly (Fig. 5(b)), then the contact angle can be 90° in the end view but is obtuse in the side view. Hence the equilibrium solution (Fig. 5(c)) is to lift the sphere slightly and impose an inward (−) deformation along $\hat{\theta}$ and an outward (+) deformation along $\hat{z}$.

2. Global deformation. While the contribution to the sum in eqn (19) from the "original" particle ($n = 0$) vanishes as $\tilde{\rho} \to \infty$, the total contribution from all other terms in the sum adds up to a net elevation. Returning to the variables $\tilde{z}, \theta$, we found:

$$\lim_{\tilde{z} \to \pm\infty} f(\tilde{z}, \theta) \approx -\frac{\delta^2}{4} \sin^4 \theta_c \cos \theta. \tag{21}$$

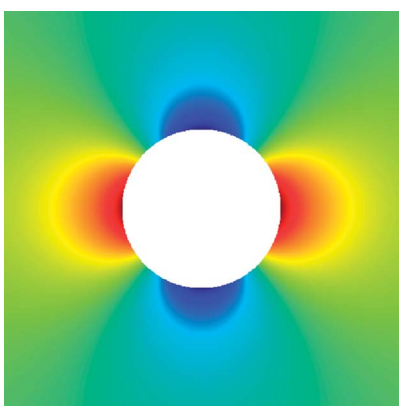

Fig. 4 Deformation of interface in the near vicinity of the particle. Red represents outward deformation; blue represents inward deformation. The orientation of the quadrupole is fixed along the direction of cylinder axis, which is horizontal in this plot.

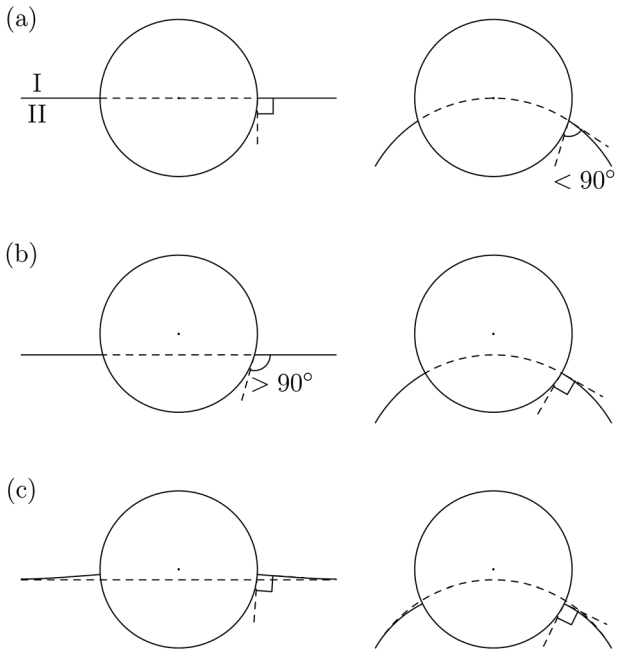

Fig. 5 Illustration of the origin of the quadrupolar deformation near the contact line as viewed from the side (left column) and along the cylinder axis (right column). (a) When the sphere is placed so that its center lies on the surface of the cylinder, $\theta_c = 90°$ along $\hat{z}$ but is acute along $\hat{\theta}$. (b) If the sphere is raised slightly, θ_c can be 90° along $\hat{\theta}$ but now θ_c is obtuse along $\hat{z}$. (c) The solution is a compromise, in which the sphere is raised and there is an inward (−) deformation along $\hat{\theta}$ and a (+) deformation along $\hat{z}$. These deformations change the curvatures in opposite ways so that H is unaffected. (The illustration exaggerates the deformation.)

This deformation corresponds to a *translation* of the cylinder by an amount $(1/4)\delta^2 \sin^4 \theta_c$ away from the center of the adsorbed particle. Again, we anticipated such a higher-order correction from the general considerations in Section II C (see eqn (12)). Notice that if one attempts to directly solve eqn (10) under the BCs ((14), (15) and (17)), the BCs at $\tilde{z} \to \pm\infty$ are not known in advance (see discussion in Section III A 2), but rather results by minimizing the energy of all deformations that satisfy $f(\tilde{z}, \theta) \propto \cos\theta$ as $\tilde{z} \to \pm\infty$.

In addition to the global translation of $O(\delta^2)$, we found also a global, higher-order, $O(\delta^4)$ tilt and undulation of the cylinder, namely, $|\tilde{z}| \cos\theta$ and $\cos\left(|\tilde{z}| - \frac{\pi}{4}\right)$ (Fig. 6). The corresponding coefficients are given in Appendix C. (Recall that the tilt is $d\zeta/dz$.)

One should notice that the translation ($O(\delta^2)$), tilt ($O(\delta^4)$), and undulations ($O(\delta^4)$) are all *zero modes* of the cylinder. Namely, these are global deformation modes that do not change the surface area of the cylinder. This is apparent for the translation and tilt modes. The undulation mode is essentially the zero-mode in the Plateau-Rayleigh spectrum of the cylinder.[43] These undulations extend along $\hat{z}$ and are required to satisfy the boundary conditions along the finite ($\hat{\theta}$) direction.

3. Near-Euclidean approximation. The above discussion suggests that one may express the deformation $f(\boldsymbol{x})$, eqn (19) as a sum of two contributions:

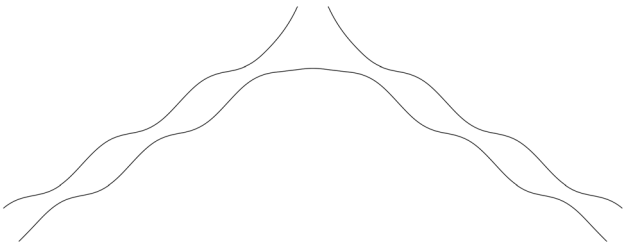

Fig. 6 Cylinder perturbed upon adsorption of solid particle, with deformation exaggerated. The actual perturbation is reduced by a factor of $\pi\delta^4\sin^4\theta_c/48$. The particle is not drawn.

$$f(\boldsymbol{x}) = f_{\text{near}}(\boldsymbol{x}) + f_{\text{far}}(\boldsymbol{x}), \tag{22}$$

where f_{near} is given in eqn (20). Let us clarify the distinction between the two functions f_{near} and f_{far}.

- The amplitude $|f_{\text{near}}(\boldsymbol{x})|$ reaches its maximal value at the contact line ($|\boldsymbol{x}| \sim a$). This maximal value remains finite ($\sim\delta^0$) as $\delta \to 0$. The function $f_{\text{near}}(\boldsymbol{x})$ decays from its maximal value as $(|\boldsymbol{x}|/a)^{-2}$, and hence vanishes as $|\boldsymbol{x}| \to \infty$.
- The amplitude $|f_{\text{far}}(\boldsymbol{x})|$ is characterized everywhere by a small value ($\sim\delta^2$) that vanishes as $\delta \to 0$, but does not decay spatially (*i.e.* as $|\boldsymbol{x}| \to \infty$). Its variation occurs over a characteristic scale H_0^{-1}.

Since in the vicinity of the particle $|f_{\text{near}}| \gg |f_{\text{far}}|$ and in addition $|f_{\text{far}}| \to 0$ everywhere as $\delta \to 0$, it is tempting to make the approximation $f(\boldsymbol{x}) \approx f_{\text{near}}(\boldsymbol{x})$. We call this the "near-Euclidean approximation," since we pointed above that f_{near} solves the Laplace equation (rather than the Helmholtz equation) if we ignore the BC (16); this approximation would describe the deformation induced by a particle with undulating contact line adsorbed on a planar interface. We will see below that this assumption cannot be made when computing the binding energy, but can nevertheless be used to compute the curvature-induced capillary force exerted on the particle.

D. Binding energy

Having calculated the interfacial deformation in the previous section, we are now in a position to evaluate the binding energy ΔE of an adsorbed particle on a cylindrical interface. Following the discussion of Section II A, we write the energy as a sum

$$\Delta E = \Delta E_{\text{cont}} + \Delta E_{\text{I–II}}. \tag{23}$$

Here we define ΔE_{cont} as the energy associated directly with the contact areas A_{I}, A_{II} of the particle with phases I, II, respectively, and the area of the hole A_{h} punched by the adsorbed particle in the fluid interface:

$$\Delta E_{\text{cont}} = -\gamma A_{\text{h}} + \gamma_1(A_{\text{I}} - 4\pi a^2) + \gamma_2 A_{\text{II}}, \tag{24}$$

The second contribution to ΔE is the energy of deforming the I–II interface:

$$\Delta E_{\text{I–II}} = \gamma \Delta A, \tag{25}$$

where ΔA is the excess area of the I–II interface induced by the deformation $\zeta(\boldsymbol{x})$ outside the contact line. Note that $\Delta A - A_{\text{h}}$ is the total change in the (infinite) area of the fluid cylindrical interface after the particle has adsorbed. We find ΔE by first evaluating ΔE_{cont} and then $\Delta E_{\text{I–II}}$.

The contribution ΔE_{cont}, eqn (24), is evaluated by noticing that the contact line can be parametrizes as $\lambda_c(\phi)$ where λ_c is the inclination angle measured from the zenith (Fig. 7). Recalling our calculation of the contact line, Section III A 1 (see eqn (12) and (13)), we find that

$$\lambda_c(\phi) = \theta_c + \frac{3-2\cos 2\phi}{6}\delta\sin\theta_c + \frac{(3-2\cos 2\phi)^2}{72}\delta^2\sin\theta_c\cos\theta_c + O(\delta^3). \tag{26}$$

An analogous parameterization of the contact line is $\rho_c(\phi)$:

$$\tilde{\rho}_c{}^2 = \delta^2\sin^2\theta_c + \frac{3-2\cos 2\phi}{3}\delta^3\sin^2\theta_c\cos\theta_c + \frac{(3-2\cos 2\phi)^2}{36}\delta^4(2-3\sin^2\theta_c)\sin^2\theta_c + O(\delta^5), \tag{27}$$

where $\tilde{\rho} = \rho/R$. Notice that the expressions (26) and (27) represent the contact line of the *perturbed* cylinder and are computed using the perturbation f, eqn (20). Our perturbative scheme (which guarantees that f is correct to $O(\delta^2)$ at the contact line), guarantees that eqn (26) and (27) are correct to orders $O(\delta^2), O(\delta^4)$, respectively. Using these parameterizations, the areas A_{I}, A_{II}, A_{h} can be expressed as:

$$\frac{A_{\text{I}}}{a^2} = \int_0^{2\pi} \mathrm{d}\phi \int_0^{\lambda_c(\phi)} \sin\lambda\,\mathrm{d}\lambda;\ A_{\text{II}} = 4\pi a^2 - A_{\text{I}} \tag{28}$$

and

$$\frac{A_{\text{h}}}{a^2} = \frac{1}{\delta^2}\left\{\frac{1}{2}\int_0^{2\pi}\mathrm{d}\phi\tilde{\rho}_c{}^2 + \frac{1}{8}\int_0^{2\pi}\mathrm{d}\phi\tilde{\rho}_c{}^4\sin^2\phi\right\} + O(\delta^4), \tag{29}$$

where the last expression is derived in Appendix D. Using eqn (24), (26)–(29) we compute the energy component (see Appendix D):

$$\Delta E_{\text{cont}} = \Delta E_{\text{flat}} + \frac{3}{16}\pi\gamma R^2\delta^4\sin^4\theta_c, \tag{30}$$

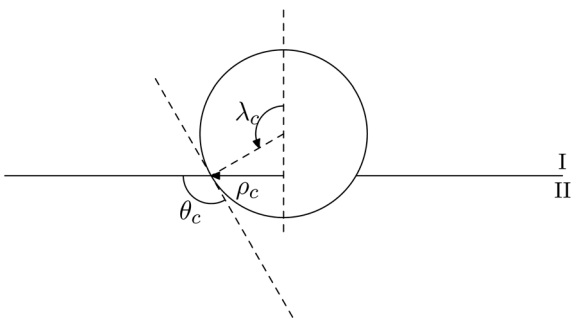

Fig. 7 Parameterizations of the contact line. Phase I is outside the cylinder and phase II is inside. ρ is the radial coordinate $\sqrt{z^2+R^2\theta^2}$. λ is the inclination angle measured from the zenith. To the lowest order, $\rho_c = a\sin\theta_c$, $\lambda = \theta_c$, corresponding to the case of flat interface.

where $\Delta E_{\mathrm{flat}} = -\pi a^2\gamma(1 + \cos\theta_c)^2$ is the binding energy of the particle on a flat interface (eqn (3)).

Next we consider the energy $\Delta E_{\mathrm{I-II}}$. We use the general formula for the area of a surface $\boldsymbol{x}(u, v)$:

$$A = \int\int |\partial_u \boldsymbol{x} \times \partial_v \boldsymbol{x}| \mathrm{d}u\mathrm{d}v, \tag{31}$$

where u,v are any set of orthogonal coordinates.[52] Expressing the perturbed cylinder through eqn (6), (8), (19), (20) and (22), we separate the above integral into a "near-Euclidean" part and a "far-field" part. These parts express the contributions to the excess area ΔA from the deformation in the vicinity of the adsorbed particle, and far away from it. The first integral is evaluated by using the coordinates $(u,v) = (\rho_0,\phi_0)$ (see eqn (18)). The second integral is computed by using the parameterization $(u,v) = (z,\theta)$. To leading order in δ we find:

$$\Delta E_{\mathrm{I-II}} = -0.5333\gamma R^2\delta^4 \sin^4\theta_c. \tag{32}$$

Combining eqn (23), (30) and (32), we find that for the case of a cylindrical interface the curvature-induced part of the binding energy is a correction of $O((aH_0)^2)$ to the binding energy to a flat interface, whose magnitude depends both on the long-range deformation as well as on the deformation in the vicinity of the contact line. Assuming this structure is characteristic of a generic CMC surface, we may conclude that with the knowledge of local surface geometry only, one cannot determine the long-range deformation and its contribution to the binding energy. Hence a general formula for the curvature-induced contribution to the binding energy in terms of the local surface geometry might not be possible. We illustrate this point in Fig. 8, which shows two hypothetical interfaces that have the same shape (thus H and G) locally but differ globally. If two such CMC interfaces exist, then the binding energy of a sphere at the point indicated in the figure would be different in the two cases.

E. Symmetry arguments

While the binding energy was obtained from explicit calculation, we will show here that the absence of $O(\delta^3)$ terms reflects the symmetries of the system. Consider then the two transformations:

I. The labels of the two fluids are switched (I $\leftrightarrow$ II) and the interface is turned "inside out" by reversing the sign of H_0 (*i.e.*, $H_0 \rightarrow -H_0$). Clearly, this transformation does not change the physical system and hence the interfacial geometry and the energy must remain invariant. Since the permutation (I $\leftrightarrow$ II) yields $\theta_c \rightarrow \pi - \theta_c$, and the sign change $H_0 \rightarrow -H_0$ implies $\delta \rightarrow -\delta$, this invariance implies that any energetic contribution that depends on δ^{2k+1} must be proportional to a function of θ_c that changes sign when $\theta_c \rightarrow \pi - \theta_c$ (*e.g.* $\cos(\theta_c)^{2n+1}$). Here n, k are any integers.

II. If the two fluids are *physically* switched so that phase I now comprises the interior of the cylinder, then a sphere will reside at the interface with a contact angle (measured from the interior of the cylinder) given by $\pi - \theta_c$. In contrast to the above transformation, this one corresponds to $\theta_c \rightarrow \pi - \theta_c$ but leaves H_0 (and hence δ) intact, hence it leads to a physically different system. Nevertheless the deformation ζ of the I–II interface is the same. This fact can be seen by noting that the BCs involve only $\sin\theta_c$ (which remains unaffected by $\theta_c \rightarrow \pi - \theta_c$). We also note that the equation for the normal vector to the fluid interface, $\hat{n}_i$ is unaffected by this change (Appendices A and B). This suggests that terms which depend on θ_c as $\sim\cos(\theta_c)^{2n+1}$ cannot appear in the energy.

As a consequence of the transformations **I**, **II**, $\Delta E_{\mathrm{I-II}}$ cannot have a term proportional to δ^3. By the first symmetry, such a term must be proportional to an odd function of $\cos\theta_c$; but this is not allowed by the second symmetry. Hence, the leading order term in $\Delta E_{\mathrm{I-II}}$ must be even in δ, as was shown in (32).

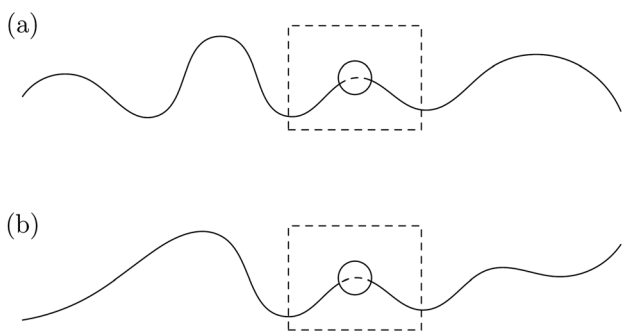

Fig. 8 Illustration of two hypothetical interfaces that have the same shape within a small region (dashed boxes) but different shapes globally. The binding energy of the sphere should in general differ in the two cases.

IV. Capillary force on one or two particles

A. Interaction between two different spheres on the cylinder

We saw in the above section that the binding energy of a particle on a curved surface cannot be obtained from a formula that depends only on the local surface geometry. However, if we now consider two small adsorbed particles, labeled "1","2", respectively, that are separated by a distance d such that $d \ll H_0^{-1}$, then the long-range deformation can be approximated by the sum $f^{(1)}_{\mathrm{far}} + f^{(2)}_{\mathrm{far}}$, which does not give rise to any interaction between the particles. However, the particles do interact through the BCs (14) at their contact lines: particle 1 induces a deformation of the surface in the vicinity of particle 2, which modifies its contact line geometry and *vice versa*. If the particles are sufficiently far from each other, such that $d \gg a$, b (where a, b are the radii of particles 1,2, respectively), then the surface deformation can be computed perturbatively:

$$f(\boldsymbol{x}) = f^{(1)}_{\mathrm{near}}(\boldsymbol{x} - \boldsymbol{x}_1) + f^{(2)}_{\mathrm{near}}(\boldsymbol{x} - \boldsymbol{x}_2) + f_{\mathrm{inter}}(\boldsymbol{x}; \boldsymbol{x}_1, \boldsymbol{x}_2) + [f^{(1)}_{\mathrm{far}}(\boldsymbol{x} - \boldsymbol{x}_1) + f^{(2)}_{\mathrm{far}}(\boldsymbol{x} - \boldsymbol{x}_2)],$$

where $\boldsymbol{x}_{1,2}$ are the locations of particles 1,2, and $|f_{\mathrm{inter}}| \ll |f^{(1,2)}_{\mathrm{near}}|$ everywhere. Following the derivations in Section III, one can compute directly f_{inter} and find the associated curvature-induced interaction energy U_{inter} between the particles. Nevertheless, we find it easier to compute the interaction by direct calculation of the capillary force.

To calculate the capillary force between the particles, we place particle 1 (with radius a) at (0, 0) and particle 2 (with radius b) at $d(\cos\omega, \sin\omega)$. At any point on the contact line of particle 1, the direction of the capillary force is parallel to the interface and perpendicular to the contact line (Fig. 9); we define the unit

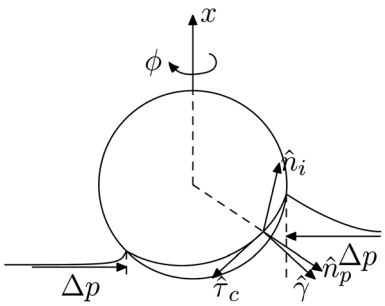

Fig. 9 Illustration of the forces on a particle. The capillary force is along the direction $\hat{\boldsymbol{t}}$, which is perpendicular to both the normal to the interface $\hat{\boldsymbol{n}}_{\mathrm{i}}$ and the tangent of the contact line $\hat{\boldsymbol{\tau}}_{\mathrm{c}}$, while $\hat{\boldsymbol{\tau}}_{\mathrm{c}}$ is perpendicular to both $\hat{\boldsymbol{n}}_{\mathrm{i}}$ and the normal to the particle surface $\hat{\boldsymbol{n}}_{\mathrm{p}}$. The pressure is greater inside the cylinder by an amount Δp, the Laplace pressure.

vector along this direction as $\hat{\boldsymbol{t}}$. By integrating around the contact line of the first particle, we obtain the capillary force exerted on particle 1:

$$\boldsymbol{F}^{(\mathrm{c})} = \int_0^{2\pi} \mathrm{d}\phi\gamma\sqrt{a^2\sin^2\theta_{\mathrm{c}} + (\partial_\phi x)^2}\,\hat{\boldsymbol{t}}(\phi), \tag{33}$$

where $\sqrt{a^2\sin^2\theta_{\mathrm{c}} + (\partial_\phi x)^2}\mathrm{d}\phi$ is the element of length along the contact line. Generally $\hat{\boldsymbol{t}}(\phi)$ is a unit vector in three dimensions, but the component along $\hat{\boldsymbol{x}}$ (Fig. 9) does not contribute to the particle–particle interaction. In the $\rho\phi$-plane, it can be shown that[50,51]

$$\hat{\boldsymbol{t}} = \hat{\boldsymbol{\rho}}\cos\psi - \frac{\partial_\phi x}{a\sin\theta_{\mathrm{c}}}\hat{\phi}\sin\psi \tag{34}$$

where $\psi = \arctan\partial\rho x$ is the angle of the interface at the contact line measured from the unperturbed interface along $\hat{\boldsymbol{\rho}}$.

Another contribution to the interaction force is the Laplace pressure γ/R across the interface (Fig. 9). One can show that the lateral component of this force in the (ρ, ϕ)-plane is

$$\boldsymbol{F}^{(\mathrm{p})} = -\frac{\gamma}{R}\int_0^{2\pi}\mathrm{d}\phi x(a\sin\theta_{\mathrm{c}},\phi)a\sin\theta_{\mathrm{c}}\hat{\boldsymbol{\rho}}, \tag{35}$$

where $x(a\sin\theta_{\mathrm{c}}, \phi)$ is the height of the contact line. In the direction along $\hat{\boldsymbol{x}}$, the Laplace pressure is balanced by the capillary force on the particle.

The total lateral force on particle 1, $\boldsymbol{F} = \boldsymbol{F}^{(\mathrm{c})} + \boldsymbol{F}^{(\mathrm{p})}$, is then obtained as

$$\boldsymbol{F}(d,\omega) = \frac{\pi\gamma a^4 b^4\sin^8\theta_{\mathrm{c}}}{3R^2d^5}\left(\hat{z}\cos 5\omega + \hat{y}\sin 5\omega\right) + O\left(\frac{\gamma a^{10}}{R^4d^5}\right), \tag{36}$$

where the correction originates from the expansion of the interfacial deformation to higher orders in a/R and b/R.

The potential energy associated with $\boldsymbol{F}$ is

$$U(d,\omega) = -\frac{\pi\gamma a^4b^4\sin^8\theta_{\mathrm{c}}\cos 4\omega}{12R^2d^4}. \tag{37}$$

This is the interaction energy between particle 1 and particle 2. Aside from the difference in sign, this interaction resembles the electrostatic interaction between two quadrupoles with fixed orientation in two dimensions (Fig. 10).[35,37]

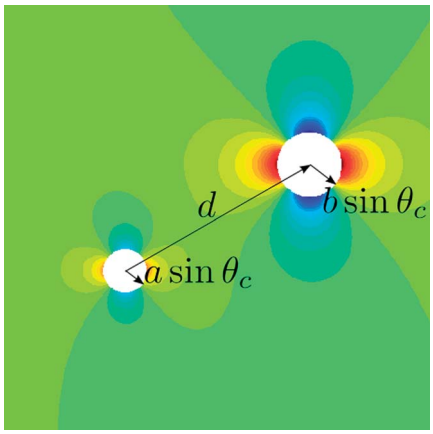

Fig. 10 Superposition of two quadrupole fields. Red represents outward deformation; blue represents inward deformation. The orientations of the quadrupoles are fixed by the direction of the cylinder axis, which is horizontal in this plot.

B. Generalization to the force on one particle at a non-uniform interface

Our result for the interaction between two different spheres at a cylindrical interface allows us to explore the more general problem of a single sphere at an interface with constant mean curvature but *non-uniform* Gaussian curvature. If we place a particle of arbitrary radius a on the cylindrical interface, the Gaussian curvature G_a caused by this perturbation at a distance $a \ll d \ll R$ can be calculated from eqn (20). In polar coordinates, if the particle a lies at (0,0), we find

$$G_a(d,\omega) = -\frac{1}{2R^2}\left(\frac{a\sin\theta_{\mathrm{c}}}{d}\right)^4\cos 4\omega + O\left(\frac{a^8}{R^2d^8}\right). \tag{38}$$

If we now envision placing a second particle with radius $b \sim a$ at position (d, ω), we can calculate the force acting on b, which we will call $\boldsymbol{F}_b$. We find the remarkable result that G_a accounts for the d, ω dependence of $\boldsymbol{F}_b$. That is, we can write

$$\boldsymbol{F}_b = -\frac{\pi\gamma b^4\sin^4\theta_c}{6}\nabla G_a + O\left(\frac{\gamma a^{10}}{R^4d^5}\right). \tag{39}$$

Correspondingly, the potential energy of particle b as a function of its position is

$$U_b(d,\omega) \approx \frac{\pi\gamma b^4\sin^4\theta_{\mathrm{c}}}{6}G_a(d,\omega), \tag{40}$$

where G_a is the Gaussian curvature of the interface *in the absence of* the particle b. This result describes in general the interaction between any two spheres on a cylinder when a, $b \ll R$. We conjecture that this result applies more generally to *any* spherical particle adsorbed on a CMC interface that initially has Gaussian curvature G_a.

In a previous study, Würger considered the case of a spherical particle on a catenoid-shaped interface ($H = 0, G < 0$).[41] He predicted that a sphere should be attracted toward the waist of the catenoid by a potential given by $-\frac{\pi}{6}\gamma a^4\sin^4\theta_{\mathrm{c}}\kappa^2$, where κ is one of the principal curvatures of the interface (the other one being $-\kappa$). Hence our result (eqn (40)), obtained with a

Table 1 Some dimensionless ratios characterizing the interfacial geometry in the present study and in that of Würger.[41] H and G should be thought of as the mean and Gaussian curvatures that exist before a test particle is inserted onto the interface

Dimensionless ratio	This article	Würger
G/H^2	$(a/d)^4 \ll 1$	$\gg 1(\to\infty)$
$\nabla G/H^3$	Ra^4/d^5	$\gg 1(\to\infty)$
$\nabla G/\lvert G\rvert^{3/2}$	$Rd/a^2 \gg 1$	$\gg 1$

cylindrical interface with $H \neq 0$, is consistent with Würger's. Our result for the cylinder with one adsorbed sphere has the additional feature of regions with both positive and negative G, which clarifies that spheres are drawn toward large negative G rather than positive G. In Table 1, we summarize the region of parameter space studied by these two works using three dimensionless ratios that characterize the interfacial shape: G/H^2, $\nabla G/H^3$, and $G/|G|^{3/2}$. In both studies, the particle size is assumed to be much smaller than any characteristic scale of the CMC surface. Würger studied the case where $H = 0$ so that G predominates. In our case, $|G| \ll H^2$ but ∇G could be either small or large compared with H^3.

As a final example of curvature-induced capillary forces, we consider the interaction between two spheres at an initially planar interface, but now with a normal force f_n acting on particle 1. As in the preceding discussion, the interface itself is not subjected to any external forces. In the presence of only particle 1, f_n causes the interface to deform into a section of a catenoid with principal curvatures κ and $-\kappa$. (In the small-deformation limit, this shape resembles a revolution of the logarithm function.) Since particle 2 – with no normal force on it – sits on a curved interface, there will be a deformation in its vicinity, which can be described to leading order in $a\kappa$ as a quadrupole. We therefore predict that particles 1 and 2 will attract one another with force

$$F = \frac{{f_n}^2 b^4 \sin^4\theta_c}{6\pi\gamma d^5}. \quad (41)$$

The same result can be obtained either by direct integration of the capillary force at the contact line (eqn (33) and (35)) or from the Gaussian curvature approach (eqn (39)).

V. Conclusions

In summary, we have shown that the adsorption of spherical particles deforms a cylindrical interface if the constant-θ_c condition applies (*i.e.*, if there is no contact-line pinning). The deformation has quadrupolar symmetry: the interface is raised along the cylinder's axis and depressed along the azimuthal directions. We find that, because of the constraint of constant mean curvature, the binding energy of a spherical particle depends on the interfacial shape far away (at scales $\gg H^{-1}$) and it appears not to be possible to write the binding energy as a function of the local G,H. In contrast, the deformation-induced interaction between two adsorbed particles can be written in terms of the local shape if the separation $d \ll H^{-1}$. Specifically, the force acting on a particle of radius b may be obtained from the gradient of the potential energy $U = \frac{\pi}{6} b^4 \sin^4\theta_c G_a$, where G_a is the Gaussian curvature induced by the other particle. Generalizing this result, we propose that this formula should describe the potential energy of a spherical particle on any CMC interface, in the limit where $b \ll H^{-1}$. Hence, spheres should generally be driven by a curvature-capillary force toward regions with more negative Gaussian curvature. The near-Euclidean approximation is misleading for calculations of the binding energy but suffices to calculate the two-particle interaction if $d \ll H^{-1}$. Our results were compared to the previous theoretical study by Würger.[41]

The magnitude of curvature-induced capillary interactions can be estimated for relevant examples using the results described here. Because of the fact that that γ is on the order of k_BT per molecular area, the interfacial tension can lead to significant force or energy when integrated over a particle that is nanometers to microns in size. (Here, k_BT is Boltzmann's constant multiplied by room temperature.) If we consider two spherical particles on a constant-mean-curvature interface, the potential energy (eqn (37)) depends on particle radius as a^2 if the geometric proportions (R/a and separation d/a) remain constant. For the case of $a = 10$ μm on an initially cylindrical interface with $R = 100a$, $d = 10a$, and $\gamma = 50$ mN m^{-1}, the potential energy is on the order of k_BT. For sub-micron spheres, the interactions are weak unless the curvature is greater or the particles are closer to one another; for example, if $a = 10$ μm, $R = 10a$ and $d = 3a$ we may obtain a potential energy on the order of $100k_BT$ and a force on the order of a femtonewton. In these cases, the curvature-induced capillary force may cause aggregation of particles in the absence of other forces. For spheres with size approaching the mm scale, buoyancy may give rise to capillary monopoles. Unless the mass density of the spheres is carefully matched to that of the liquids, these capillary monopoles may compete with the curvature-induced capillary interactions.

The formalism described here opens a way to study curvature effects on CMC interfaces with *arbitrary* shape. The linear operator in eqn (7) can be used in analytical or numerical studies as long as the deformation is small. An interesting case, not described here, would be for two particles that are far apart on the interface, *i.e.*, when the separation d approaches the characteristic scale of the curvature, H^{-1}. On the other hand, the very highly curved limit where $H^{-1} \sim a$ requires a different approach because the mean curvature becomes a nonlinear function of the deformation and the starting Helmholtz equation (10) is already incorrect. The limit where $d \sim a$ is also challenging because the contact-line boundary conditions are no longer satisfied to leading order by linear superposition of the two single-particle deformations.

An interesting remaining problem is how these curvature-capillary forces apply in the presence of gravity or other external forces. We showed that a neutrally buoyant particle is attracted to another particle that is subject to a normal force f_n because f_n induces a quadrupolar deformation around the neutrally buoyant particle. However, when there is an external force that acts on the interface itself, H is no longer constant and the force on a particle might have additional terms proportional to ∇H, *etc.* In the present work, we effectively assumed that all characteristic lengths are much smaller than

the capillary length $\sqrt{\gamma/(\Delta\rho g)}$, where $\Delta\rho$ is the difference in mass densities of the two fluids and g is the acceleration due to gravity. In the case of liquid–air interfaces, the capillary length is typically on the order of millimeters, so that neglecting gravity should be a good approximation when considering microscopic particles. For large particles or for external forces stronger than gravity, a generalization to the case of non-uniform H would be interesting and quite useful in many applications.

Appendix A: CMC deformation of a cylinder

Here we provide a straightforward derivation of the operator that describes the change in the mean curvature upon a small deformation of a cylinder of radius R. We use the definition of the mean curvature in terms of the normal to the surface:

$$2H = \nabla\hat{n}, \tag{A1}$$

to obtain directly the CMC deformation of a cylindrical surface. With eqn (5) and (6) we can obtain the equation for the perturbation $\zeta = a\delta f$ where a is a length (*e.g.* the radius of the adsorbed particle) and $\delta = a/R \ll 1$. The normal is related to the gradient of the surface equation

$$\Phi(r,\theta,z) = r - R - a\delta f(\theta,z), \tag{A2}$$

by the relation:

$$\hat{\boldsymbol{n}} = \frac{\nabla\Phi}{|\nabla\Phi|}. \tag{A3}$$

We have

$$\nabla\Phi = \left(1, -\frac{a\delta}{r}\partial_\theta f, -a\delta\partial_z f\right). \tag{A4}$$

We define now the dimensionless variables as in the main text: $\tilde{r} = r/R$ and $\tilde{z} = z/R$. The gradient can then be written as

$$\nabla\Phi = \left(1, -\frac{\delta^2}{\tilde{r}}\partial_\theta f, -\delta^2\partial_{\tilde{z}} f\right). \tag{A5}$$

Consequently

$$|\nabla\Phi| = 1 + O(\delta^4). \tag{A6}$$

At the lowest order in δ, we have that $\hat{\boldsymbol{n}} = \nabla\Phi$. The normal is computed on the perturbed surface $\tilde{r} = 1 + \delta^2 f$. Thus we have at the lowest order

$$\frac{1}{\tilde{r}} = 1 - \delta^2 f. \tag{A7}$$

Finally

$$\hat{\boldsymbol{n}} = (1, -\delta^2\partial_\theta f, -\delta^2\partial_{\tilde{z}} f) \tag{A8}$$

$$\nabla\hat{\boldsymbol{n}} = \frac{1}{r}\partial_r(rn^r) + \frac{1}{r}\partial_\theta n^\theta + \partial_z n^z = \frac{1}{R\tilde{r}} - \frac{\delta^2}{R\tilde{r}}\partial_\theta{}^2 f - \frac{\delta^2}{R}\partial_{\tilde{z}}{}^2 f$$
$$= \frac{1}{R} - \frac{\delta^2}{R}f - \frac{\delta^2}{R}\partial_\theta{}^2 f - \frac{\delta^2}{R}\partial_{\tilde{z}}{}^2 f, \tag{A9}$$

where we used eqn (A7). Using eqn (5) together with eqn (A1) and $H_0 = 1/(2R)$, we obtain

$$2\delta H = -\delta^2(1 + \partial_\theta{}^2 + \partial_{\tilde{z}}{}^2)f \tag{A10}$$

As discussed in the main text, $\delta H = 0$ and we thus obtain the Helmholtz equation (10).

Appendix B: boundary condition at contact

The boundary condition we search for is given by

$$\hat{\boldsymbol{n}}_{\mathrm{p}}\cdot\hat{\boldsymbol{n}}_{\mathrm{i}} = \cos\theta_{\mathrm{c}}, \tag{B1}$$

where $\hat{\boldsymbol{n}}_{\mathrm{p}}$ and $\hat{\boldsymbol{n}}_{\mathrm{i}}$ are the normal of the particle surface and fluid interface, respectively. To leading order in δ,

$$\hat{\boldsymbol{n}}_{\mathrm{p}} = \left(\cos\theta_{\mathrm{c}} + \delta f + \frac{\theta^2}{2\delta}, \frac{\theta}{\delta}, \frac{\tilde{z}}{\delta}\right), \tag{B2}$$

$$\hat{\boldsymbol{n}}_{\mathrm{i}} = (1, -\delta^2\partial_\theta f, -\delta^2\partial_{\tilde{z}} f), \tag{B3}$$

where we express the above vectors using cylindrical coordinates (see Fig. 2). It then follows that:

$$f - \theta\partial_\theta f - \tilde{z}\partial_{\tilde{z}} f = -\frac{\theta^2}{2\delta^2}. \tag{B4}$$

Appendix C: summation of series

For given $\tilde{z}$ and θ, the sum to be approximated is:

$$S = s_0 + \sum_{n=1}^{\infty}(s_n + s_{-n}), \tag{C1}$$

where

$$s_n = [J_2(\rho_n) + Y_2(\rho_n)]\cos 2\phi_n. \tag{C2}$$

Numerical summation is done by computing a partial sum directly and approximating the remainder.

In the limit of large n, Taylor expansion yields

$$s_n + s_{-n} = \frac{A(\tilde{z},\theta)}{n^{3/2}} + \frac{B(\tilde{z},\theta)}{n^{7/2}} + O\left(\frac{1}{n^{9/2}}\right), \tag{C3}$$

where

$$A(\tilde{z},\theta) = \frac{4\theta\sin\theta - (4\tilde{z}^2 + 15)\cos\theta}{4\sqrt{2}\pi^2}, \tag{C4}$$

$$B(\tilde{z},\theta) = \frac{\left[4\tilde{z}^2(16\tilde{z}^4 + 1140\tilde{z}^2 + 4275) - 720\theta^2(4\tilde{z}^2 + 15) - 945\right]\cos\theta - 60\theta\left(16\tilde{z}^4 + 408\tilde{z}^2 - 16\theta^2 + 105\right)\sin\theta}{6144\sqrt{2}\pi^4}. \tag{C5}$$

The mean curvature is computed using eqn (A1). We need to compute the divergence of the normal vector.

For sufficiently large n,

$$s_n + s_{-n} \approx \frac{A(\theta, \tilde{z})}{n^{3/2}}, \tag{C6}$$

which requires

$$n^2 \gg \left|\frac{B}{A}\right|. \tag{C7}$$

Now the approximation is

$$S \approx s_0 + \sum_{n=1}^{N} \left(s_n + s_{-n} - \frac{A}{n^{\frac{3}{2}}} \right) + A\zeta\left(\frac{3}{2}\right) \tag{C8}$$

with $\zeta(x)$ the Riemann zeta function.

The sum was computed at different points in the $(\tilde{z},\theta)$ plane and the data showed the leading modes of S correspond to a kink followed with an undulation (Fig. 6):

$$S = .6371|\tilde{z}|\cos\theta - .4502\cos\left(|\tilde{z}| - \frac{\pi}{4}\right) + \xi(\tilde{z},\theta). \tag{C9}$$

The equation above was obtained by fitting data in the quadrant of positive $\tilde{z}$ and θ. The symmetry condition was shown by taking explicitly the absolute values of $\tilde{z}$ and θ. The remainder $\xi(\tilde{z},\theta)$ would contribute to the binding energy.

Appendix D: the area A_h

The area A_h of the hole is a part of the cylinder which is curved. To compute this area, we use the cylindrical system of coordinate used in the paper, see Fig. 2. The parametric equation of the cylinder is thus

$$\tilde{x} = \cos\theta;\ \tilde{y} = \sin\theta;\ \tilde{z} = \tilde{z}, \tag{D1}$$

with $\tilde{\ } = \cdot/R$, with $0 \le \theta < 2\pi$ and $-\infty < \tilde{z} < \infty$. We thus use this parameterization for the hole

$$\tilde{\boldsymbol{r}}(\theta,\tilde{z}) = (\cos\theta,\ \sin\theta,\ \tilde{z}). \tag{D2}$$

Using polar coordinates

$$\tilde{z} = \tilde{\rho}\cos\phi, \tag{D3}$$

$$\theta = \tilde{\rho}\sin\phi, \tag{D4}$$

and eqn (13) which characterizes the region occupied by the particle on the cylinder, we find (up to corrections of $O(\delta^2)$):

$$\tilde{\boldsymbol{r}}(\tilde{\rho},\phi) = \left(1 - \frac{1}{2}\tilde{\rho}^2\sin^2\phi, \tilde{\rho}\sin\phi, \tilde{\rho}\cos\phi\right). \tag{D5}$$

Using the general formula for the surface area we find:

$$\frac{A_h}{R^2} = \int_0^{2\pi} d\phi \int_0^{\tilde{\rho}_c} d\tilde{\rho} \left|\partial_{\tilde{\rho}}\tilde{\boldsymbol{r}} \times \partial_{\phi}\tilde{\boldsymbol{r}}\right|, \tag{D6}$$

from which follows that:

$$\frac{A_h}{R^2} = \int_0^{2\pi} d\phi \int_0^{\tilde{\rho}_c} d\tilde{\rho}\tilde{\rho}\left(1 + \frac{1}{2}\tilde{\rho}^2\sin^2\phi\right) + O(\delta^6), \tag{D7}$$

$$\frac{A_h}{R^2} = \frac{1}{2}\int_0^{2\pi} d\phi \tilde{\rho}_c{}^2 + \frac{1}{8}\int_0^{2\pi} d\phi \tilde{\rho}_c{}^4\sin^2\phi + O(\delta^6). \tag{D8}$$

Using now eqn (27) we compute the integrals in the above equation and obtain eqn (29). Finally, a similar computation of the integral for A_I in eqn (26) shows that terms of $O(\delta^3)$ cancel and we obtain the expression for the energy component ΔE_{cont}, eqn (30).

Acknowledgements

The authors thank Christian Santangelo for insightful discussions related to this work. Support from Materials Research Science and Engineering Center DMR-0820506 and the National Science Foundation CBET-0967620 is greatly appreciated. We also acknowledge partial support for CZ and ADD by the Polymer-Based Materials for Harvesting Solar Energy, an Energy Frontier Research Center funded by the U.S. Department of Energy, Office of Science, Office of Basic Energy Sciences under Award Number DE-SC0001087. FB thanks the Government of the Region of Wallonia (REMANOS Research Programs) for financial support.

References

1 A. Bhargava, A. V. Francis and A. K. Biswas, *J. Colloid Interface Sci.*, 1978, **64**, 214.
2 A. P. Sullivan and P. K. Kilpatrick, *Ind. Eng. Chem. Res.*, 2002, **41**, 3389.
3 M. H. Ese, C. M. Selsbak, A. Hannisdal and J. Sjoblom, *J. Dispersion Sci. Technol.*, 2005, **26**, 145–154.
4 J. Sun and X. L. Zheng, *J. Environ. Monit.*, 2009, **11**, 1801.
5 H. P. Zhang, M. Khatibi, Y. Zheng, K. Lee, Z. K. Li and J. V. Mullin, *Mar. Pollut. Bull.*, 2010, **60**, 1433.
6 S. U. Pickering, *J. Chem. Soc.*, 1907, 2001.
7 R. G. M. van der Sman and A. J. van der Goot, *Soft Matter*, 2009, **5**, 501.
8 O. D. Velev, K. Furusawa and K. Nagayama, *Langmuir*, 1996, **12**, 2374.
9 A. D. Dinsmore, M. F. Hsu, M. G. Nikolaides, M. Marquez, A. R. Bausch and D. A. Weitz, *Science*, 2002, **298**, 1006.
10 Y. Lin, H. Skaff, T. S. Emrick, A. D. Dinsmore and T. P. Russell, *Science*, 2003, **299**, 226.
11 Y. Lin, H. Skaff, A. Baker, A. D. Dinsmore, T. Emrick and T. P. Russell, *J. Am. Chem. Soc.*, 2003, **125**, 12690.
12 H. Duan, D. Wang, D. G. Kurth and H. Mohwald, *Angew. Chem., Int. Ed.*, 2004, **43**, 5639.
13 A. B. Subramaniam, M. Abkarian and H. A. Stone, *Nat. Mater.*, 2005, **4**, 553.
14 C. Zeng, H. Bissig and A. D. Dinsmore, *Solid State Commun.*, 2006, **139**, 547.
15 K. Stratford, R. Adhikari, I. Pagonabarraga, J. C. Desplat and M. E. Cates, *Science*, 2005, **309**, 2198.
16 E. M. Herzig, K. A. White, A. B. Schofield, W. C. K. Poon and P. S. Clegg, *Nat. Mater.*, 2007, **6**, 966.
17 K. Du, E. Glogowski, T. Emrick, T. P. Russell and A. D. Dinsmore, *Langmuir*, 2010, **26**, 12518.
18 P. Pieranski, *Phys. Rev. Lett.*, 1980, **45**, 569.
19 A. F. Koretsky and P. M. I. Kruglyakov, *Izv. Sib. Otd. Akad. Nauk SSSR, Ser. Khim. Nauk*, 1971, **2**, 139.
20 M. Oettel, A. Dominguez and S. Dietrich, *Phys. Rev. E: Stat., Nonlinear, Soft Matter Phys.*, 2005, **71**, 051401.
21 M. M. Nicolson, *Proc. Cambridge Philos. Soc.*, 1949, **45**, 288.
22 D. Y. C. Chan, J. D. Henry and L. R. White, *J. Colloid Interface Sci.*, 1981, **79**, 410.
23 D. Vella and L. Mahadevan, *Am. J. Phys.*, 2005, **73**, 817.
24 V. N. Paunov, B. P. Binks and N. P. Ashby, *Langmuir*, 2002, **18**, 6946.

25 M. G. Nikolaides, A. R. Bausch, M. F. Hsu, A. D. Dinsmore, M. P. Brenner, C. Gay and D. A. Weitz, *Nature*, 2002, **420**, 299.
26 M. G. Nikolaides, A. R. Bausch, M. F. Hsu, A. D. Dinsmore, M. P. Brenner, C. Gay and D. A. Weitz, *Nature*, 2003, **424**, 1014.
27 M. Megens and J. Aizenberg, *Nature*, 2003, **424**, 1014.
28 A. Dominguez, M. Oettel and S. Dietrich, *J. Chem. Phys.*, 2007, **127**, 204706.
29 A. Würger, *Europhys. Lett.*, 2006, **75**, 978.
30 J. Guzowski, M. Tasinkevych and S. Dietrich, *Eur. Phys. J. E*, 2010, **33**, 219.
31 A. Dominguez, M. Oettel and S. Dietrich, *EPL*, 2007, **77**.
32 A. Würger, *EPL*, 2007, **77**, 68003.
33 J. C. Loudet, A. M. Alsayed, J. Zhang and A. G. Yodh, *Phys. Rev. Lett.*, 2005, **94**, 018301.
34 M. M. Müller, M. Deserno and J. Guven, *Phys. Rev. E: Stat., Nonlinear, Soft Matter Phys.*, 2005, **72**, 061407.
35 A. Dominguez, M. Oettel and S. Dietrich, *J. Chem. Phys.*, 2008, **128**, 114904.
36 E. P. Lewandowski, M. Cavallaro, L. Botto, J. C. Bernate, V. Garbin and K. J. Stebe, *Langmuir*, 2010, **26**, 15142.
37 K. D. Danov, P. A. Kralchevsky, B. N. Naydenov and G. Brenn, *J. Colloid Interface Sci.*, 2005, **287**, 121.
38 D. Stamou, C. Duschl and D. Johannsmann, *Phys. Rev. E: Stat., Nonlinear, Soft Matter Phys.*, 2000, **62**, 5263.
39 U. Srinivasan, M. A. Helmbrecht, C. Rembe, R. S. Muller and R. T. Howe, *IEEE J. Sel. Top. Quantum Electron.*, 2002, **8**, 4.
40 R. J. Knuesel and H. O. Jacobs, *Proc. Natl. Acad. Sci. U. S. A.*, 2010, **107**, 993.
41 A. Würger, *Phys. Rev. E: Stat., Nonlinear, Soft Matter Phys.*, 2006, **74**, 041402.
42 P. A. Kralchevsky and K. Nagayama, *Particles at Fluid Interfaces and Membranes*, Elsevier Science B.V., Amsterdam, The Netherlands, 2001.
43 P. de Gennes, F. Brochard-Wyart and D. Quere, *Capillary and Wetting Phenomena – Drops, Bubbles, Pearls, Waves*, Springer, 2002.
44 B. Davidovitch, D. Ertaş and T. C. Halsey, *Phys. Rev. E: Stat., Nonlinear, Soft Matter Phys.*, 2004, **70**, 031609.
45 J. M. Dimeglio and E. Raphael, *J. Colloid Interface Sci.*, 1990, **136**, 581.
46 S. Komura, Y. Hirose and Y. Nonomura, *J. Chem. Phys.*, 2006, **124**, 241104.
47 P. A. Kralchevsky, V. N. Paunov, N. D. Denkov and K. Nagayama, *J. Colloid Interface Sci.*, 1994, **167**, 47.
48 O. D. Velev, N. D. Denkov, V. N. Paunov, P. A. Kralchevsky and K. Nagayama, *J. Colloid Interface Sci.*, 1994, **167**, 66.
49 H. Lehle and M. Oettel, *Phys. Rev. E: Stat., Nonlinear, Soft Matter Phys.*, 2007, **75**, 011602.
50 P. A. Kralchevsky and K. Nagayama, *Adv. Colloid Interface Sci.*, 2000, **85**, 145.
51 P. A. Kralchevsky, V. N. Paunov, N. D. Denkov, I. B. Ivanov and K. Nagayama, *J. Colloid Interface Sci.*, 1993, **155**, 420.
52 B. O'Neill, *Elementary Differential Geometry*, Academic Press, 1997.

